Pseudomonas aeruginosa Contains a Novel Type V Porphobilinogen Synthase with No Required Catalytic Metal Ions†

Nicole Frankenberg,‡ Dieter Jahn,*,‡ and Eileen K. Jaffe§

Institut für Organische Chemie und Biochemie, Albert-Ludwigs-Universität, Albertstrasse 21, 79104 Freiburg im Breisgau, Germany, and Institute for Cancer Research, Fox Chase Cancer Center, 7701 Burholme Avenue, Philadelphia, Pennsylvania 19111

Received March 19, 1999; Revised Manuscript Received June 7, 1999

ABSTRACT: Porphobilinogen synthases (PBGS) are metalloenzymes that catalyze the first common step in tetrapyrrole biosynthesis. The PBGS enzymes have previously been categorized into four types (I−IV) by the number of Zn^{2+} and/or Mg^{2+} utilized at three different metal binding sites termed A, B, and C. In this study *Pseudomonas aeruginosa* PBGS is found to bind only four Mg^{2+} per octamer as determined by atomic absorption spectroscopy, in the presence or absence of substrate/product. This is the lowest number of bound metal ions yet found for PBGS where other enzymes bind 8−16 divalent ions. These four Mg^{2+} allosterically stimulate a metal ion independent catalytic activity, in a fashion dependent upon both pH and K^+. The allosteric Mg^{2+} of PBGS is located in metal binding site C, which is outside the active site. No evidence is found for metal binding to the potential high-affinity active site metal binding sites A and/or B. *P. aeruginosa* PBGS was investigated using Mn^{2+} as an EPR probe for Mg^{2+}, and the active site was investigated using [3,5-^{13}C]porphobilinogen as an NMR probe. The magnetic resonance data exclude the direct involvement of Mg^{2+} in substrate binding and product formation. The combined data suggest that *P. aeruginosa* PBGS represents a new type V enzyme. Type V PBGS has the remarkable ability to synthesize porphobilinogen in a metal ion independent fashion. The total metal ion stoichiometry of only 4 per octamer suggests half-sites reactivity.

Porphobilinogen synthases (PBGS,[1] EC 4.2.1.24) are homooctameric enzymes that catalyze an early step in tetrapyrrole biosynthesis. The reaction, illustrated in Figure 1, is the conversion of two molecules of 5-aminolevulinic acid (ALA) to the monopyrrole precursor porphobilinogen, which is further oligomerized to form tetrapyrroles such as heme, chlorophyll, or corrins (*1*). The two substrates are called A-side ALA and P-side ALA according to their fate in the product.

All PBGS that have been purified and characterized to date are metalloenzymes that require Mg^{2+}, Zn^{2+}, or both for catalysis. This functional diversity is reflected by structural differences within putative metal binding motifs (*2*). In general, the Zn^{2+}-dependent enzymes are characterized by highly conserved cysteine and histidine residues for the coordination of the metal while Mg^{2+}-dependent enzymes possess carboxylic acid containing residues instead (*3, 4*). Interestingly, some PBGS's are stimulated by monovalent cations whose binding site(s) remain(s) unknown (*5, 6*). On the basis of these characteristics a further subclassification for Mg^{2+}- and Zn^{2+}-dependent PBGS's was suggested which includes four types of enzymes that differ in their ability to bind divalent cations at three different sites (*6*). The metal ions of PBGS can function either catalytically or allosterically.

Pseudomonas aeruginosa PBGS has been established to be a Mg^{2+} utilizing PBGS with activity independent of Zn^{2+} (*7*). Like some other PBGS's, the activity also responds to monovalent cations such as potassium. On the basis of an initial inspection of the potential metal binding sequences and the degree of amino acid identity to the *Bradyrhizobium japonicum* PBGS, our initial presumption was that *P. aeruginosa* PBGS is a type IV protein. Type IV PBGS's contain 12 metal ions, with 4 at the active sites and 8 at allosteric sites (*6*).

The stoichiometry of metal ions on *B. japonicum* PBGS and bovine PBGS suggests half-sites reactivity for these enzymes (*6, 8*). The concept of half-sites reactivity for PBGS containing four functional active sites per octamer was first suggested in 1973 (*9*) but continues to be discussed controversially. *Escherichia coli* PBGS is one example; it has been reported to possess eight A-side ALA binding sites and eight P-side ALA binding sites per octamer (*10*) while other reports demonstrate only four *functional* active sites per *E. coli* PBGS octamer (*11, 12*). The published crystal structures of yeast and *E. coli* PBGS indeed show eight equivalent TIM barrels, each apparently containing an active site (*13, 14*).

† This work was supported by the Deutsche Forschungsgemeinschaft (Ja 470/3-4, Ja 470/5-1), Sonderforschungsbereich 388, Albert-Ludwigs-Universität Freiburg, Fonds der Chemischen Industrie, and NIH Grant ES03654 (E.K.J.). N.F. was also supported by a Smith Kline Beecham Stiftung and a short-time fellowship of Boehringer Ingelheim Fonds.

* To whom correspondence should be addressed. Tel: +49-761-2036060. Fax: +49-761-2036096. E-mail: jahndiet@uni-freiburg.de.

§ Albert-Ludwigs-Universität.

‖ Fox Chase Cancer Center.

[1] Abbreviations: PBGS, porphobilinogen synthase; ALA, 5-aminolevulinic acid; EDTA, ethylenediaminetetraacetic acid; TES, *N*-[tris(hydroxymethyl)methyl]-2-aminoethanesulfonic acid; NMR, nuclear magnetic resonance; EPR, electron paramagnetic resonance.

10.1021/bi9906470 CCC: $18.00
Published on Web 10/01/1999

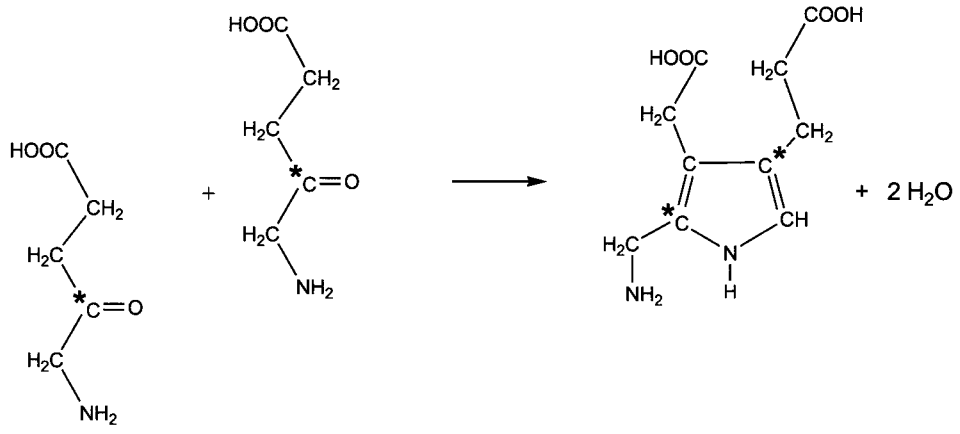

FIGURE 1: PBGS-catalyzed reaction. In an asymmetric condensation two molecules of ALA form porphobilinogen, the precursor for all tetrapyrroles. The two substrate molecules are called A-side ALA and P-side ALA according to whether they contribute respectively to the acetyl- or propionyl-containing halves of porphobilinogen. The asterisks mark the ^{13}C labels for ^{13}C NMR studies.

Here we describe the detailed characterization of the numbers and functions of the Mg^{2+} of *P. aeruginosa* PBGS. The unexpected results lead to the proposal that *P. aeruginosa* represents a new type V PBGS with the unusual ability to catalyze the formation of porphobilinogen in a metal ion independent fashion.

MATERIALS AND METHODS

Materials. All chemicals were purchased from Sigma, Deisenhofen, Germany, or Sigma, St. Louis, MO, and were ACS grade or better. Glacial acetic acid and 70% perchloric acid were purchased from Riedel-de-Haen, Seelze, Germany. Centricon-10 concentrator devices were purchased from Amicon as were PM10 membranes used in stirred pressure cell concentrators.

Protein Methods. Production and purification of *P. aeruginosa* PBGS were performed as described by the accompanying paper (*7*). The kinetic assays in this work followed the protocols of Petrovich et al. (*6*). High protein concentrations were obtained using a 3 mL stirred pressure cell at 30 psi (Amicon).

Dependence of PBGS Activity on Mg^{2+} Concentration at Different pH Values and Potassium Availability. PBGS was dialyzed overnight against 100 mM bis-tris propane-HCl, pH 8.2, which resulted in a drastic decrease of enzymatic activity (~4% residual activity); the dialyzed protein was determined to be essentially metal free by atomic absorption spectroscopy. This was designated apo-PBGS. Different Mg^{2+} concentrations prepared in the same buffer were added to the enzyme and assayed using 35 μg/mL PBGS in the assay and a fixed ALA-HCl concentration of 10 mM. The stopped reaction mixtures were diluted as necessary with a 2:1 mixture of buffer and 20% TCA prior to treatment with Ehrlich's reagent to keep the absorption in the linear range (<1.0). Under these conditions, the lowest A_{555} values obtained were in the range of 0.15 and were obtained with a high degree of precision. The Mg^{2+} dependence of the activity was determined at pH values of 6.5, 6.9, and 8.2 in the presence and absence of 100 mM KCl. The pH 8.2 Mg^{2+} activation curve was also obtained at 16 and 22 °C because temperature has been seen to effect metal binding to other PBGS proteins (unpublished results). The data were analyzed by a least-squares best fit using the program Kaleidagraph (Abelbeck Software) to equations described in Results and Discussion.

Determination of Mg^{2+} Binding by Atomic Absorption Spectroscopy. Metal ion stoichiometry was determined by atomic absorption using a Perkin-Elmer Analyst 100 flame spectrometer. All binding experiments were carried out in 100 mM bis-tris propane-HCl, and 100 mM KCl, pH 8.2. For preliminary ultrafiltration experiments, the initial PBGS concentration was 10 μM subunits mixed with 20 μM ALA and 40 μM Mg^{2+}. After 15 min incubation at 22 °C, free and bound metals were separated by ultrafiltration using Centricon-10 devices at 4 °C. The enzyme solution was quantified for protein and Mg^{2+} content, and the effluent was quantified for Mg^{2+}. Similar experiments were carried out at 37 °C using 20 μM PBGS subunits and Mg^{2+} concentrations varying from 10 to 40 μM and a prewarmed rotor.

For equilibrium dialysis experiments 100 μL of PBGS (35 mg/mL, ~1 mM subunits) was dialyzed against 250 mL of 100 mM bis-tris propane-HCl, 100 mM KCl, and 1 mM $MgCl_2$, pH 8.2, in the presence or absence of 10 mM levulinic acid or 10 mM ALA-HCl. Samples were dialyzed at 22 °C for 16 h and diluted 1:50 prior to protein concentration determination and atomic absorption analysis.

^{13}C NMR Studies. ^{13}C NMR spectra were obtained at 75.45 MHz on a Bruker AM300 spectrometer using a 45° pulse angle and 2 s recycle time. To minimize the rotational correlation time of this 300 KDa protein, the sample temperature was regulated at 37 °C (*15*). Proton decoupling was utilized; blocks of 4000 scans were obtained; and 8−11 blocks were obtained per sample. To prepare the sample, 1.4 mL of PBGS (56 mg/mL) was mixed with 0.3 mL of D_2O. Subsequently, [4-^{13}C]ALA (see Figure 1) was added at a ratio of 1 equiv per enzyme subunit followed by successive addition of $MnCl_2$ and EDTA to final concentrations of 2 and 15 mM, respectively. ^{13}C NMR spectra were obtained after each addition. Protein was recovered by dialysis against 2 × 1 l 50 mM TES−KOH, pH 6.7, for 8 h, followed by overnight dialysis against 2 L of 100 mM TES−KOH, pH 8.2, to obtain apo-PBGS, which had full activity when assayed in the presence of $MgCl_2$.

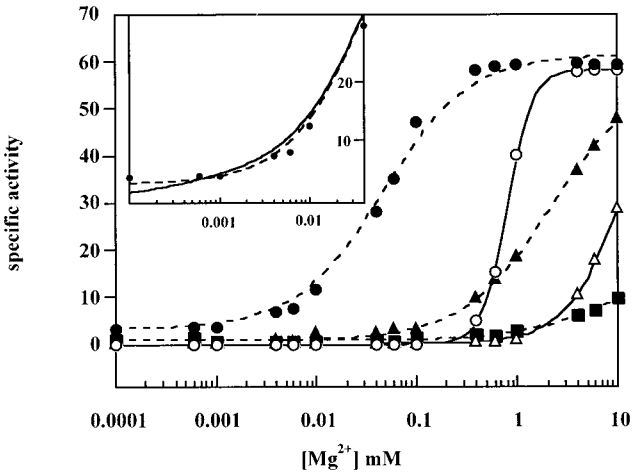

FIGURE 2: Mg^{2+} dependence of *P. aeruginosa* PBGS activity as a function of pH and K^+ in the buffer bis-tris propane at 10 mM ALA-HCl and 35 μg/mL enzyme. Closed symbols represent assays done in the presence of 100 mM KCl; assays done in the absence of KCl are shown as open symbols. The pH values are (○) pH 8.2, (Δ) pH 6.9, and (□) pH 6.5. The solid line represents the best fit to eq 1. Dashed lines represent the fits to eq 3. The insert in the upper left corner is an enlargement of the pH 8.2 curve fits to eqs 2 (solid line) and 3 (dashed line) between 0 and 0.04 mM $MgCl_2$. The kinetic parameters are included in Table 1.

Mn^{2+} Electron Paramagnetic Resonance Studies. X-band (9.14 GHz) EPR spectra were obtained on a computer-interfaced Varian E-109 spectrometer. The data acquisition was at 22 °C with spectrometer settings of 50 mW microwave power, 8 G modulation amplitude, and a sweep rate of 250 G/min; four scans were averaged. Prior to EPR, apo-PBGS was thoroughly dialyzed against 100 mM TES−KOH, pH 8.2, and concentrated to ~2 mM subunits. Matched samples were prepared at various concentrations of Mn^{2+} (25−500 μM) with and without 2 mM ALA; the final protein concentration was 64 mg/mL.

RESULTS

PBGS Activity as a Function of Mg^{2+} Concentration. Prior studies showed that *P. aeruginosa* PBGS activity responds to $Mg^{2+}$and not Zn^{2+} (*7*). To identify the role(s) of Mg^{2+} in *P. aeruginosa* PBGS, Mg^{2+} activation was investigated as a function of pH in the buffer bis-tris propane-HCl in the presence and absence of potassium. We have already established that K^+ activates *P. aeruginosa* PBGS and followed the work of Petrovich et al. (*6*), who showed that both the divalent and monovalent metal ion activations of *B. japonicum* PBGS were dependent upon pH. Figure 2 illustrates the Mg^{2+} dependence of *P. aeruginosa* PBGS at pH 8.2, 6.9, and 6.5 in the presence and absence of 100 mM KCl. The Mg^{2+} activation curves obtained for the *P. aeruginosa* PBGS look remarkably similar to those of *B. japonicum* PBGS, which was found to bind four catalytically essential Mg^{2+} and eight allosteric Mg^{2+} (*6*). Without potassium the data fit to a cooperative binding model that can be described by eq 1 (the solid lines in Figure 2). This

$$\text{specific activity} = \frac{V'[\text{Mg}]^n}{K_{\text{d(req)}}{}^n + [\text{Mg}]^n} \qquad (1)$$

model is characterized by a maximal rate V', a single K_d for Mg^{2+}, and a Hill coefficient n. Table 1 shows these values at pH 8.2 and 6.9. At pH 6.5 the enzyme shows virtually no activity without K^+ even at 10 mM Mg^{2+}.

Table 1: Kinetic Parameters Describing the Mg^{2+} Activation of *P. aeruginosa* PBGS As Illustrated in Figure 2[a]

pH	temp (°C)	100 mM K^+	V^* (μmol mg^{-1} h^{-1})	V′ (μmol mg^{-1} h^{-1})	$K_{d(act)}$ (mM)	activation factor	app Hill coef
6.5	37	+	0.76		7	20.0×	
6.9	37	−		48.7			1.8
6.9	37	+	0.84		2.1	67.0×	
8.2	37	−		58.2			3.5
8.2	37	+	3.2		0.046	19.0×	
	22	+	0.2		0.47	92.0×	
	16	+	0.2		1.90	48.0×	

[a] All kinetic constants derived from data obtained in the presence of potassium were obtained by fitting to eq 3. In the absence of potassium the kinetic constants were deduced using eq 1.

In the presence of potassium the data can be fitted to a two-site model with an essential Mg^{2+} and an allosteric Mg^{2+} described by eq 2. V^0 describes enzyme activity in the

$$\text{specific activity} = \frac{V^0[\text{Mg}]}{K_{\text{d(req)}} + [\text{Mg}]} + \frac{((V^0a) - V^0)[\text{Mg}]}{K_{\text{d(act)}} + [\text{Mg}]} \qquad (2)$$

presence of one required Mg^{2+}, and a is an activation factor derived from a second, allosteric Mg^{2+}. $K_{d(req)}$ and $K_{d(act)}$ are dissociation constants for these two Mg^{2+}, respectively. This model provided an excellent fit for *B. japonicum* PBGS under these conditions (*6*). In the case of *P. aeruginosa* PBGS at pH 8.2, eq 2 provides a good description of data obtained at Mg^{2+} concentrations above 40 μM, where $K_{d(req)} < 0.4$ μM, V^0 is 3.9 μmol h^{-1} mg^{-1}, $K_{d(act)}$ is 47 μM, and the activation factor is 15-fold upon binding the allosteric Mg^{2+}. These parameters are close to those obtained for *B. japonicum* PBGS and predict the existence of a very tight binding Mg^{2+} in the presence of substrate or product (*6*). However, eq 2 gives a poor fit to the data in the presence of potassium at low Mg^{2+} concentrations (Figure 2 insert, solid line). Hence, a third model was considered where *P. aeruginosa* PBGS binds only an allosteric Mg^{2+} that stimulates a divalent metal ion independent catalytic activity. This is described by eq 3, where V^* is the metal-independent rate and K_d describes

$$\text{specific activity} = V^* + \frac{((V^*a) - V^*)[\text{Mg}]}{K_{\text{d}} + [\text{Mg}]} \qquad (3)$$

the binding of an allosteric Mg^{2+}. The values for these kinetic constants are given in Table 1 at pH 8.2, 6.9, and 6.5, and the best-fit lines are included in Figure 2 (dashed lines). Although eqs 2 and 3 fit the data equally well at higher Mg^{2+} concentrations, and provide approximately the same kinetic constants for the allosteric Mg^{2+}, eq 3 gives a superior fit to the low [Mg^{2+}] data (Figure 2 insert, dashed lines). The difference between these two models lies in the inclusion of a high-affinity ($K_d \ll \mu$M) Mg^{2+} binding site. Thus, discrimination between these two models can be based on the experimental determination of the total stoichiometry and affinity of Mg^{2+} ions for *P. aeruginosa* PBGS as described below.

In the course of the outlined Mg^{2+} activation studies, we also discovered a large temperature dependence of the Mg^{2+} activation profiles. This temperature dependence of the kinetic parameters is included in Table 1 for pH 8.2 in the presence of potassium. The dramatically reduced metal ion affinity with decreasing temperature suggests that metal binding contributes to the large Arrhenius coefficients that have been documented for other PBGS (*11, 13, 16*).

Determination of the Number of Mg^{2+} Binding Sites. To experimentally examine the existence of a high-affinity metal binding site in *P. aeruginosa* PBGS, ultrafiltration studies were performed at Mg^{2+} concentrations below the apparent K_d for the allosteric Mg^{2+} at pH 8.2 in the presence of potassium. These studies were carried out in the presence of substrate/product because the apparently analogous tight-binding Mg^{2+} site of *B. japonicum* PBGS only exists under these conditions (*6, 17*). Room temperature binding measurements under these conditions revealed enzyme-bound Mg^{2+} at less than one per octamer. The experiments were repeated at 37 °C, and again the maximum amount of bound metal detected was no more than one Mg^{2+} per octamer. These data provide no evidence in support of a high-affinity Mg^{2+} binding site in *P. aeruginosa* PBGS.

Total Mg^{2+} stoichiometry under conditions that saturate the allosteric Mg^{2+} site was determined by equilibrium dialysis at 1 mM total Mg^{2+} (pH 8.2 plus potassium; see Figure 2) and 1 mM enzyme subunits in the presence and absence of substrate or the substrate analogue levulinic acid. Under these conditions the apparent $K_{d(act)}$ for the allosteric Mg^{2+} is ~50 μM; thus stoichiometric binding is expected when the concentrations of both enzyme and Mg^{2+} are at 1 mM and the Mg^{2+} is in a 250-fold molar excess over enzyme subunits. In all cases, the total amount of enzyme-bound Mg^{2+} was 4.0 $\pm$ 0.5 per octamer. This remarkable result reveals an extraordinarily low amount of total divalent metal, in fact the lowest determined for any PBGS yet described.

The Mg^{2+} binding data combined with the Mg^{2+} activation studies discriminate between the two models described by eqs 2 and 3. Equation 2 requires the presence of a high-affinity Mg^{2+} binding site in addition to the allosteric Mg^{2+} site. In the case of *B. japonicum* PBGS this high-affinity site existed only in the presence of substrate or product *(6, 17)*. The binding experiments presented here exclude a high-affinity metal binding in the presence or absence of substrate or product and are not consistent with the model described by eq 2. The marginal amount of Mg^{2+} present at low [Mg^{2+}] is consistent with subsaturating occupancy of the allosteric Mg^{2+} site. The binding data and the kinetic data are consistent with the model described by eq 3 where the four enzyme-bound Mg^{2+} correspond to the allosteric activation phenomenon. Several significant conclusions arise from a stoichiometry of 4 allosteric Mg^{2+} per octamer and no tightly bound Mg^{2+} even under conditions that support catalysis. Most importantly, this establishes that, at low [Mg^{2+}], *P. aeruginosa* PBGS can slowly catalyze the formation of porphobilinogen in a metal ion independent fashion. It suggests that the *P. aeruginosa* PBGS active site does not contain divalent metal ions even under conditions of maximal activity. Second, this suggests that the protein uses only four functional monomers per octamer at any one time, a concept known as half-sites reactivity. The newly revealed crystal structure of *P. aeruginosa* PBGS provides additional support for the concept of half-sites reactivity (see Discussion).

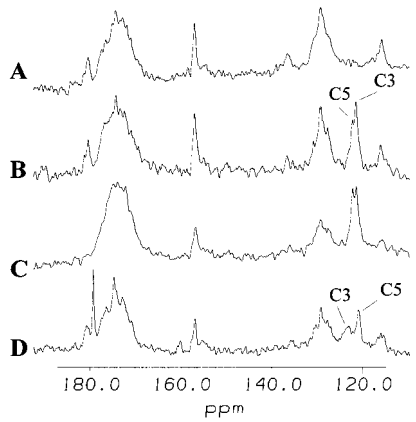

FIGURE 3: sp and sp^2 regions of the ^{13}C NMR spectra of [3,5-^{13}C]-porphobilinogen and PBGS complexes. Spectrum A represents *P. aeruginosa* PBGS. The sample contained 1.7 mL of 46 mg/mL protein in 100 mM bis-tris propane-HCl, 10 mM $MgCl_2$, 100 mM KCl, pH 8.2, and 21% (v/v) D_2O. There were 44 000 transients. Spectrum B shows [3,5-^{13}C]porphobilinogen bound to *P. aeruginosa* PBGS. 18 μL of 100 mM [4-^{13}C]ALA was added to the previous sample; 32 000 transients were collected. Spectrum C shows the effect of adding Mn^{2+} (35 μL of 91 mM $MnCl_2$) to the previous sample. There were 36 000 transients. Spectrum D shows the effect of adding EDTA (25.5 μL of 1 M EDTA, pH 8.0) to the previous sample; 36 000 transients were collected.

Evaluation of the Kinetic Consequences of Binding the Allosteric Mg^{2+}. Experiments were performed to quantify the allosteric effect of Mg^{2+} on the residual 4% metal-independent PBGS activity. Earlier studies of *E. coli* PBGS showed that the allosteric Mg^{2+} caused a 10-fold reduction in the K_m for ALA (at neutral pH), a 2-fold increase in V_{max}, and an increased affinity for the required Zn^{2+} (*18*). Hence we determined the K_m and V_{max} values for *P. aeruginosa* PBGS in the presence and absence of Mg^{2+}. The protein was exhaustively dialyzed against pH 8 buffer until no residual Mg^{2+} was detectable. Then K_m and k_{cat} values were determined in the presence and absence of 10 mM Mg^{2+}. Mg^{2+} dramatically reduced the K_m for ALA from 4.2 to 0.3 mM. Mg^{2+} increased the value of k_{cat} 25-fold from 0.05 to 1.26 s^{-1}, the later of which corresponds to a maximal specific activity of 60 μmol h^{-1} mg^{-1} and is calculated on the basis of four active sites per octamer. These allosteric effects of Mg^{2+} on *P. aeruginosa* PBGS mirror those of *E. coli* and *B. japonicum* PBGS (*6, 18*). In support of the identification of the Mg^{2+} of *P. aeruginosa* PBGS as comparable to the allosteric Mg^{2+} of *E. coli* PBGS, we previously showed that both stabilize the octamer against electrophoretic separation (*7, 18*).

^{13}C NMR To View Porphobilinogen Bound at the Enzyme Active Site. A *P. aeruginosa* PBGS active site that is free of divalent metal ions is quite different from other PBGS we have characterized. Thus, we undertook ^{13}C NMR studies to view the active site using ^{13}C-labeled substrate/product. The natural abundance ^{13}C NMR spectrum of the enzyme is shown in Figure 3A; it contains no unexpected features and resembles those obtained for the other PBGS (*11, 15, 17*). The addition of [4-^{13}C]ALA (see Figure 1) yields the immediate conversion to [3,5-^{13}C]porphobilinogen whose ^{13}C NMR resonances are seen to arise at 122.8 and 121.6 ppm (Figure 3B). This spectrum is identical to that seen for *B.*

japonicum PBGS where a mixed labeling experiment identified the signals as arising from C3 and C5, respectively (*17*). The identity of the two spectra extends to the asymmetry of the carbon resonance intensities, the upfield signal appearing slightly less intense.

The addition of Mn^{2+} to the *P. aeruginosa* enzyme−product complex had a remarkable effect on the ^{13}C NMR spectra as seen in Figure 3C. Consistent with expectations, the free carboxyl resonances from the protein (∼180 ppm) are broadened significantly. Quite unexpectedly, the aromatic resonances derived from the protein are also significantly broadened (reduced in intensity) (115−140 ppm region) relative to the backbone carbonyl region (165−178 ppm). In contrast, the enzyme-bound porphobilinogen signals are NOT dramatically broadened, a strong indication that the Mn^{2+} does not reside in the active site. On the other hand, the addition of Mn^{2+} has a subtle effect on the resonances from enzyme-bound porphobilinogen as the signals are seen to lose their asymmetry. One possible explanation for this could lie in a long-distance paramagnetic relaxation effect, which shortens the relaxation times and overcomes an asymmetric saturation phenomenon since our 2 s recycle time does not allow for complete relaxation between magnetic pulses.

The final spectrum, shown in Figure 3D, was obtained after the addition of sufficient EDTA to chelate all the divalent metal ions. The chemical shifts of product revert to those seen for free product (121.0 and 123.0 ppm for C5 and C3, respectively), but the line widths remain broad and the asymmetry in peak height returns. The latter characteristics suggest the enzyme-bound state. One possible interpretation for this result is that the chemical environment returns to one resembling bulk solvent while the product remains bound. This result is in contrast to that seen for mammalian, *E. coli*, and *B. japonicum* PBGS; the addition of metal chelating agents to the enzyme−product complex causes the release of product from the active site and a concomitant narrowing of the ^{13}C resonances.

Taken together, these results are consistent with the interpretation that the active site of *P. aeruginosa* PBGS is different from PBGS previously explored using [3,5-^{13}C]-porphobilinogen as an active site probe. However, the similarity between the spectra of enzyme-bound [3,5-^{13}C] porphobilinogen of *P. aeruginosa* PBGS and *B. japonicum* PBGS was unexpected and suggests the need for a refined interpretation of the data for the latter system (see Discussion).

Mn^{2+} EPR as a Probe of the Mg^{2+} Binding Sites. The kinetic, metal binding, and NMR studies present a consistent picture of *P. aeruginosa* PBGS as containing no active site metals. To further explore this novel result, we look from the perspective of the enzyme-bound Mg^{2+} using Mn^{2+} as an EPR probe. Mn^{2+} has chemical properties similar to those of Mg^{2+} and as such serves as an excellent paramagnetic probe for Mg^{2+} binding sites on proteins (*19*). Mn^{2+} has previously been used to view and quantify the allosteric Mg^{2+} sites of *E. coli* PBGS (*18*), and for *B. japonicum* PBGS, Mn^{2+} EPR provided the definitive proof of two different Mg^{2+} environments (*17*).

To ensure that Mn^{2+} EPR is a valid probe for *P. aeruginosa* PBGS, we determined that Mn^{2+} functionally substitutes for Mg^{2+}. The apparent $K_{d(act)}$ was found to be 32 μM, and the activation factor was 22-fold for Mn^{2+} activation of *P. aeruginosa* PBGS in 100 mM TES−KOH buffer at pH 8.0. These values nicely mimic those seen for Mg^{2+} under comparable conditions (see Table 1) and allow us to apply Mn^{2+} EPR to the study of *P. aeruginosa* PBGS.

The enzyme-bound Mn^{2+} EPR spectra showed a typical six-line pattern, somewhat broader than free Mn^{2+} in the same buffer and considerably reduced in intensity (data not shown). The preparation of matched samples containing substrate/product caused no detectable change in the intensity of line width of the EPR spectra. No changes were detected even under conditions where only 10% of the total Mn^{2+} sites were saturated (75 μM Mn^{2+} and 1.6 mM subunits). Thus, the addition of substrate does not change either the affinity or the environment of the Mn^{2+} probe. Similar observations were made using EPR spectroscopic analysis of *E. coli* PBGS where Mg^{2+} coordination was also independent of substrate or product (*18*). This is in sharp contrast to *B. japonicum* PBGS where the addition of substrate was seen to cause a disproportionation of subsaturating Mn^{2+} from the allosteric Mg^{2+} site to the catalytic Mg^{2+} site (*17*).

P. aeruginosa PBGS Defines a New Type V PBGS. Our model describing the variation in metal ion usage by PBGS is illustrated in Figure 4. This model differentiates three different types of divalent metal binding sites called A, B, and C, which coordinate Me_A, Me_B, and Me_C (*2, 6, 20*). On the basis of prior work, Me_A functions at the active site to facilitate A-side ALA binding and reactivity (*21*); the ligands to Me_B have been proposed to be involved in C_5 proton removal from P-side ALA (*2*). The A and B nomenclature originated with EXAFS studies of the two Zn^{2+} of bovine PBGS and is based on the derived ligands (mostly oxygen and nitrogen for Zn_A and mostly sulfur for Zn_B) (*22*). Me_C is an allosteric activator and has been proposed to bind at subunit interfaces outside the active site (*11, 18, 20*). Figure 4 includes the total divalent metal stoichiometries and the proposed stoichiometries of the metals at each of the three sites. Figure 4 also incorporates a correlation to an alternative model that includes only two different types of sites called Meα and Meβ (*23*). The former model considers half-sites reactivity while the latter model does not. Inherent in both of these models is the assumption that all PBGS's have an absolute requirement for a divalent metal ion. The current work identifies the constellation of metal ions of *P. aeruginosa* PBGS as different from all PBGS's previously characterized. Thus *P. aeruginosa* PBGS is denoted type V PBGS. Type V PBGS disproves the assumption that all PBGS's require divalent cations and raises the interesting question of what active site components can functionally substitute for Me_A and Me_B.

DISCUSSION

The new information about *P. aeruginosa* PBGS has been used to refine the three metal ion model for all PBGS's as illustrated in Figure 4. Historically, the existence, location, and functions of Me_A, Me_B, and Me_C were deduced on the basis of sequence comparisons, conserved structural characteristics, kinetic measurements, chemical modification studies, metal determination experiments, and NMR and EPR studies (*2*−*4, 6, 11, 17, 21, 24*−*26*). Recently, the existence

Type	Species	Metal ions required for full activity per homooctamer				Metal site with ligands to Me_A and Me_B	Metal site with ligands to Me_A and Me_C	Refs.
		Site A	Site B	Site C	Total metals			
I	*H. sapiens*	4 Zn	4 Zn	Absent	8	AC**C**VG**C**LG**C**PYTSHGH**C**GLLSE	DRR**C**YQL.PPGARGLALRAV	*(4)*
?	*S. cerevisiae*	8 Zn	8 Zn	Absent	16	IC**C**VG**C**LG**C**EYTSHGH**C**GVLYD	DRK**C**YQL.PPAGRGLARRAL	*(29)*
II	*E. coli*	4 Zn or Absent	4 Zn or 8 Znα	8 Mg	16	MS**C**TG**C**G**C**EYTSHGH**C**GVL**C**E	DRKSYQMNPMN.RREAIR**C**S	*(11, 20, 27)*
				8 Mgβ	16			
III	*P. sativum*	4 Mg or Absent	4 Mg or 8 Mgα	8 Mg	16	YT**C**VAL**C**PYSS**C**GH**C**GIVRE	DKKTYQMNPAN.YREALT**C**M	*(28)*
				8 Mgβ	16			
IV	*B. japonicum*		4 Mg	8 Mg	12	LG**C**VAL**C**PFTSHGH**C**GLIAD	DKRTYQMDSAN.TDEALR**C**V	*(6)*
	P. aeruginosa	Absent	Absent	4 Mg	4	IT**C**VAL**C**PFTTHGQ**C**GILDD	NKATYQMDPAN.SDEALH**C**V	
Metal Ligands According to Biochemical Analysis & Crystal Structures						* * ** B B AB	* * A C	*(2, 13, 14, 30)*

FIGURE 4: Updated three metal ion model for PBGS including the stoichiometry of the various metal ions at the different sites (see references). Two regions of the PBGS sequence are illustrated that have been shown to be involved in metal ion binding. Doubly underlined amino acid residues represent regions of metal ion binding postulated on the basis of primary sequence information/comparisons (*3, 4, 20*). The asterisks indicate where X-ray crystallography has established ligands to Zn_A, Zn_B, and Mg_C; the metal sites are listed below the asterisks (*13, 14*). Ligands have not yet been established for Mg_A or Mg_B or whether these comparable sites exist. The binding of 16 metals to *E. coli* PBGS has been interpreted in two different ways (*11, 18, 23, 27*), both of which are included. A fundamental difference between these two models is the number of functional active sites per octamer. The binding of 16 Mg^{2+} to pea (*Pisum sativum*) PBGS (*28*) is also presented with two possible interpretations. For yeast (*Saccharomyces cerevisiae*) PBGS, the total metal binding has been shown to be 16 per octamer (*29*), and the crystal structure shows two enzyme-bound Zn^{2+} whose ligands agree with those predicted for Zn_A and Zn_B (*13, 20*). If this assignment proves to be correct, then yeast PBGS identifies yet another type of PBGS.

of all three sites has been established by X-ray crystallography (*13, 14*), and the ligands show a remarkable correlation to those predicted (*20*). However, not all three sites have been detected on one single enzyme.

The crystal structure of yeast PBGS shows two different active site Zn^{2+} (Me_A and Me_B) drawing ligands from a cysteine- and histidine-rich region of sequence illustrated in column 4 of Figure 4 (*4, 13*). The ligands derived from the crystal structure are noted in the figure. A potential Mg^{2+} binding domain in plant enzymes was postulated in the same region having aspartic acid residues in the position of some Zn^{2+} binding domain cysteine and histidine residues (*3*). No PBGS crystal structures have as yet placed Mg^{2+} bound to this region of the sequence. However, elegant cassette mutagenesis studies that delete the plant-like sequence and insert the human sequence demonstrated a shift from a Mg^{2+}-dependent enzyme to a Zn^{2+}-dependent enzyme (*24*). Alignment of the deduced amino acid sequence of *P. aeruginosa* PBGS with other PBGS sequences initially suggested a potential Mg^{2+} binding motif in this active site region of the sequence (*7*). The current results, indicating that *P. aeruginosa* PBGS does not require Mg^{2+} bound to this region, suggest that the aspartates of this region, without the need for a coordinated Mg^{2+}, can functionally substitute for the cysteines that are coordinated to Zn_B.

The sequence of *P. aeruginosa* PBGS is most like *B. japonicum* PBGS, which has been found to contain four tight-binding active site Mg^{2+} per octamer in addition to eight allosteric Mg^{2+} (*6*). These were assigned as 4 Mg_A and 8 Mg_C. The similarity of the chemical shifts of enzyme-bound [3,5-^{13}C]porphobilinogen for these two proteins suggests a refinement of our model for *B. japonicum* PBGS. One must appreciate that the ^{13}C chemical shifts of isotopically labeled substrates, products, or inhibitors bound to enzyme active sites provide information about the chemical environment of the active site. ^{13}C NMR has previously been used to view [3,5-^{13}C]porphobilinogen bound to PBGS from mammals, *E. coli*, and *B. japonicum* (*11, 15, 17*). These enzymes share a pairwise sequence identity of approximately 35%. When identical chemical shifts were observed for [3,5-^{13}C]porphobilinogen bound to mammalian and *E. coli* PBGS, the similarity was interpreted to reflect the presence of Zn^{2+} at the active site for both of these enzymes. Because Zn_A is proposed to be directly coordinated to porphobilinogen (*2*), this interaction was deemed responsible for the large chemical shift effects that were observed. In contrast, *B. japonicum* PBGS exhibits rather small shifts for this labeled product. This was interpreted as an environmental difference on the basis of the substitution of Mg_A for Zn_A. In keeping with this interpretation, the replacement of the paramagnetic Mn^{2+} for Mg^{2+} significantly broadened the ^{13}C resonances of product bound to *B. japonicum* PBGS (*17*); paramagnetic broadening is not seen for product bound to *E. coli* PBGS, which uses Mg^{2+} only in the Me_C site (*18*). The identity of the spectrum of product bound to *P. aeruginosa* PBGS with that of *B. japonicum* PBGS suggests that no metal is directly

bound to product on the latter protein and alters the previous interpretation. This is consistent with ENDOR studies that failed to show an interaction between [^{15}N]porphobilinogen and Mn^{2+} at the active site of *B. japonicum* PBGS (Petrovich, LoBrutto, and Jaffe, unpublished results). Thus, since Me_A is proposed to be product bound, the four active site Mg^{2+} of *B. japonicum* PBGS are reassigned to the Me_B site as included in Figure 4.

During the course of these studies the crystal structure of *P. aeruginosa* PBGS in complex with levulinic acid (LA) was solved (*30*). The octameric enzyme consists of four *asymmetric* dimers. One monomer of each dimer is found to contain a Mg^{2+} that is located close to the surface in the vicinity of the N-terminal extended arm of the second monomer. The known active site amino acids are found in the central cavity at the C-terminal end of the $(\beta\alpha)_8$ barrel. The Mg^{2+}-bound monomer is found with a "closed" lid sealing the active site. For the other monomer the active site lid is partially disordered. In the metal-free active site LA is seen bound analogous to a Schiff base intermediate that forms between the P-side ALA molecule with an active site lysine (*31*). It is the other, A-side ALA molecule that is believed associated with the active site metal ion (*2*). Hence, the crystal structure established the location of the four allosteric Mg^{2+} but left open the possibility of an active site Mg^{2+}. The current work establishes that, under optimal enzymic activity, the allosteric Mg^{2+} seen in the crystal structure are the only divalent metal ions present.

In conclusion, the results presented herein indicate that *P. aeruginosa* PBGS defines a new type V PBGS protein. It is the first known PBGS where it has been proven that the formation of porphobilinogen does not have an absolute requirement for either zinc or magnesium. The type V protein contains only four magnesium ions per octamer, the lowest stoichiometry for metal ions in PBGS proteins studied so far, and provides a strong indication for half-sites reactivity in this homooctameric protein. The remarkable variation in metal ion usage at the active sites of the various types of PBGS suggests substantial variations in the details of the catalytic mechanism and identifies the metabolically essential PBGS as a potential drug target.

ACKNOWLEDGMENT

We thank Dr. G. D. Markham for his help with the EPR spectroscopic studies.

REFERENCES

1. Jordan, P. M. (1991) Biosynthesis of Tetrapyrroles, *New Compr. Biochem. 19*, 1−66.
2. Jaffe, E. K. (1995) *J. Bioenerg. Biomembr. 27*, 169−179.
3. Boese, Q. F., Spano, A. J., Li, J. M., and Timko, M. P. (1991) *J. Biol. Chem. 266*, 17060−17066.
4. Wetmur, J. G., Bishop, D. F., Cantelmo, C., and Desnick, R. J. (1986) *Proc. Natl. Acad. Sci. U.S.A. 83*, 7703−7707.
5. Nandi, D. L., and Shemin, D. (1973) *Arch. Biochem. Biophys. 158*, 305−311.
6. Petrovich, R. M., Litwin, S., and Jaffe, E. K. (1996) *J. Biol. Chem. 271*, 8692−8699.
7. Frankenberg, N., Heinz, D., and Jahn, D. (1999) *Biochemistry 38*, 13968−13975.
8. Bevan, D. R., Bodlaender, P., and Shemin, D. (1980) *J. Biol. Chem. 255*, 2030−2035.
9. Cheh, A. (1973) Ph.D. Dissertation, University of California, Berkeley.
10. Spencer, P., and Jordan, P. M. (1995) *Biochem. J. 305*, 151−158.
11. Mitchell, L. W., and Jaffe, E. K. (1993) *Arch. Biochem. Biophys. 300*, 169−177.
12. Mitchell, L. W., Volin, M., and Jaffe, E. K. (1995) *J. Biol. Chem. 270*, 24054−24059.
13. Erskine, P. T., Senior, N., Awan, S., Lambert, R., Lewis, G., Tickle, I. J., Sarwar, M., Spencer, P., Thomas, P., Warren, M. J., Shoolingin-Jordan, P. M., Wood, S. P., and Cooper, J. B. (1997) *Nat. Struct. Biol. 4*, 1025−1031.
14. Erskine, P. Y., Norton, E., Cooper, J. B., Lambert, R., Coker, A., Lewis, G., Spencer, P., Sarwar, M., Wood, S. P., Warren, M. J., and Shoolingin-Jordan, P. M. (1999) *Biochemistry 14*, 4266−4276.
15. Jaffe, E. K., and Markham, G. D. (1987) *Biochemistry 26*, 4258−4264.
16. Schlösser, M., and Beyersmann, D. (1987) *Biol. Chem. Hoppe-Seyler 368*, 1469−1477.
17. Petrovich, R. M., and Jaffe, E. K. (1997) *Biochemistry 36*, 13421−13427.
18. Jaffe, E. K., Ali, S., Mitchell, L. W., Taylor, K. M., Volin, M., and Markham, G. D. (1995) *Biochemistry 34*, 244−251.
19. Reed, G., and Markham, G. (1984) in *Biological Magnetic Resonance* (Reuben, L. J. B. A. J., Ed.) pp 73−142, Plenum Press, New York and London.
20. Jaffe, E. (1993) *Commun. Inorg. Chem. 15*, 67−93.
21. Jaffe, E. K., Abrams, W. R., Kaempfen, H. X., and Harris, K. A., Jr. (1992) *Biochemistry 31*, 2113−2123.
22. Dent, A. J., Beyersmann, D., Block, C., and Hasnain, S. S. (1990) *Biochemistry 29*, 7822−7828.
23. Spencer, P., and Jordan, P. M. (1993) *Biochem. J. 290*, 279−287.
24. Chauhan, S., and O'Brian, M. R. (1995) *J. Biol. Chem. 270*, 19823−19827.
25. Jaffe, E. K., Volin, M., Myers, C. B., and Abrams, W. R. (1994) *Biochemistry 33*, 11554−11562.
26. Jaffe, E. K., and Hanes, D. (1986) *J. Biol. Chem. 261*, 9348−9353.
27. Spencer, P., and Jordan, P. M. (1994) *Biochem. J. 300*, 373−381.
28. Senior, N. M., Brocklehurst, K., Cooper, J. B., Wood, S. P., Erskine, P., Shoolingin-Jordan, P. M., Thomas, P. G., and Warren, M. J. (1996) *Biochem. J. 320*, 401−412.
29. Senior, N. M., Siligardi, G., Drake, A., Thomas, P. G., and Warren, M. J. (1997) *Biochem. Soc. Trans. 25*, 78S.
30. Frankenberg, N., Erskine, P. T., Cooper, J. B., Shoolingin-Jordan, P. M., Jahn D., and Heinz, D. W. (1999) *J. Mol. Biol. 289*, 591−602.
31. Jordan, P. M., and Sheera, J. S. (1980) *FEBS Lett. 114*, 283−286.

BI9906470